



# A $\text{Au}_{82}\text{Si}_{18}$ liquid metal field-ion emitter for the production of Si ions: fundamental properties and mechanisms

L. Bischoff<sup>a</sup>, G.L.R. Mair<sup>b</sup>, C. J. Aidinis<sup>b,\*</sup>, C.A. Londos<sup>b</sup>,  
C. Akhmadaliev<sup>a</sup>, Th. Ganetsos<sup>b</sup>

<sup>a</sup> *Research Center Rossendorf Inc, Institute of Ion Beam and Materials Research, P.O. Box 510119, D-01314 Dresden, Germany*

<sup>b</sup> *Department of Physics, University of Athens, Section of Applied Physics, Panepistimiopolis, Zographos, GR-15784 Athens, Greece*

Received 13 August 2003; received in revised form 10 December 2003; accepted 26 January 2004

## Abstract

Focused silicon beams are useful for direct write applications, e.g., lithography on silicon without the undesirable effect of substrate contamination. However, since pure silicon is not amenable to liquid metal ion source (LMIS) manufacture, a suitable alloy containing silicon has to be produced. This paper covers almost all fundamental aspects of a  $\text{Au}_{82}\text{Si}_{18}$  eutectic, including the most detailed beam mass spectra reported to date of a AuSi source. A finding worthy of note in this investigation, manifested in the behaviour of the ion extraction voltage with temperature, is the abnormal behaviour of the surface tension coefficient of the alloy with temperature. An important deduction from this work, however, concerns the mechanisms responsible for the creation of doubly charged ions: reasons of self-consistency indicate that while  $\text{Si}^{2+}$  is directly field evaporated,  $\text{Au}^{2+}$  must form by the post-ionization of  $\text{Au}^+$ . Finally, two different mechanisms seem to co-exist, as far as the production of cluster ions is concerned. While for cluster ions containing only a few atoms some sort of surface field-ionization mechanism might be responsible for their creation, for larger clusters, a droplet break-up mechanism, possibly by ion capture, seems very likely.

© 2004 Elsevier B.V. All rights reserved.

PACS: 7.77.Ka; 79.70.+q

Keywords: Silicon ions; Liquid metal ion source; Field evaporation

The study of AuSi liquid metal alloy ion sources (LMAISs) is not new. Different researchers have investigated different aspects of such sources. Machelet et al. [1], e.g., studied the mass spectra of a  $\text{Au}_{82}\text{Si}_{18}$  source, but for the current range they considered the source acts more like a droplet sprayer rather than like an ion source. The present

work encompasses almost all fundamental aspects of a  $\text{Au}_{82}\text{Si}_{18}$  source.

Focused Si ion beams are useful for direct write applications, e.g. lithography on Si substrates without substrate contamination. As we shall see later, Si ions-producing sources emit these ions mostly in a doubly charged state. This means that a given ion energy can be achieved with half the accelerating voltage that would be required for singly charged ions. However Si tends to react chemically with most needle substrates and this is

\*Corresponding author. Tel.: +30-1072-76712; fax: +30-1072-76801.

E-mail address: [caidinis@cc.uoa.gr](mailto:caidinis@cc.uoa.gr) (C.J. Aidinis).

the reason why Si liquid metal ion sources (LMISs) usually employ a suitable alloy containing Si. The Si ions are subsequently mass separated from the beam, by, e.g., an ExB filter, as in the present case. Amongst other reasons why an alloy has to be employed in certain cases are a high melting point and vapour pressure of the metal of interest. The  $\text{Au}_{82}\text{Si}_{18}$  eutectic used in this work has the reasonably low melting point of  $365^\circ\text{C}$ .

Fig. 1 shows a current–voltage ( $i$ – $V_0$ ) curve of the source. The curve is linear and steeply rising, typical of well-wetted, well-roughened or grooved needles [2]. The voltage has to be raised by  $\sim 2\%$  above the source starting ( $V_{\text{OC}}$ ) or extinction ( $V_{\text{OX}}$ ) voltage to reach  $30\ \mu\text{A}$  emission current. In other words, and especially for low currents,  $V_0$  differs only marginally from  $V_{\text{OC}} \simeq V_{\text{OX}}$ , where [3].

$$V_{\text{OC}} \propto \gamma^{1/2}, \quad (1)$$

$\gamma$  being the surface tension coefficient of the liquid metal, or alloy. With most elemental sources and some liquid metal alloy ion sources,  $\gamma$  decreases linearly with temperature ( $T$ ), which is translated into a similar behaviour [4] of  $V_{\text{OC}}$ , provided changes in  $\gamma$  are small—as they normally are [5]. This is not the case, however, with the alloy under consideration. From Fig. 2 it is seen that  $V_0$ , i.e.  $\gamma$ , at first increases, reaches a broad maximum and then it decreases. This behaviour was first reported with a  $\text{Au}_{77}\text{Ge}_{14}\text{Si}_9$  source [4] (Fig. 2) and an explanation was then given in terms of a residual crystalline structure at the surface of the liquid alloy. The rising portion of the curve corresponds

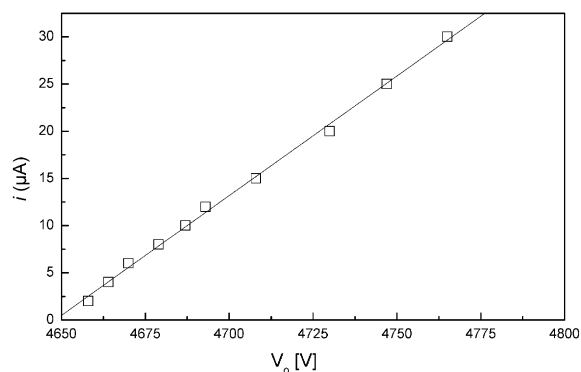


Fig. 1. Current–voltage ( $i$ – $V_0$ ) characteristics of  $\text{Au}_{82}\text{Si}_{18}$  source for  $T=730^\circ\text{C}$ .

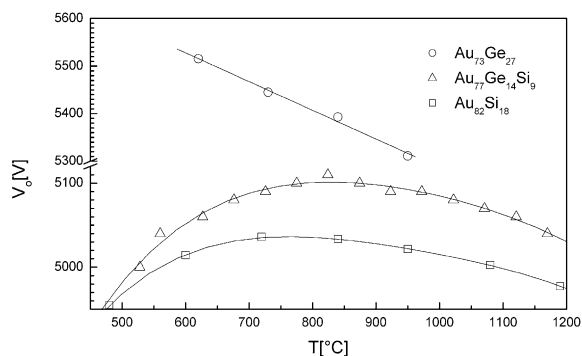


Fig. 2. Extraction voltage ( $V_0$ ) versus emitter temperature ( $T$ ) for  $\text{Au}_{73}\text{Ge}_{27}$ ,  $\text{Au}_{77}\text{Ge}_{14}\text{Si}_9$  and  $\text{Au}_{82}\text{Si}_{18}$  LMIS. Current,  $i=10\ \mu\text{A}$ .

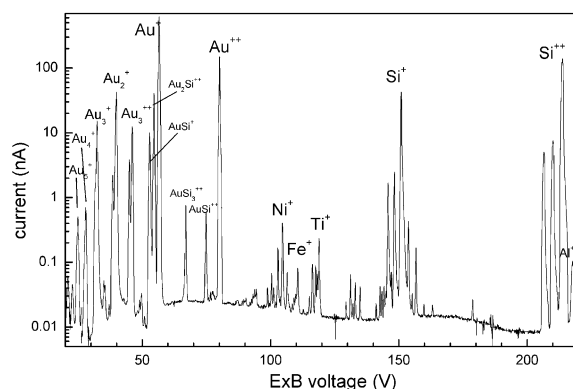


Fig. 3. Mass spectrum of  $\text{Au}_{82}\text{Si}_{18}$  source for  $T=850^\circ\text{C}$ ,  $i=4\ \mu\text{A}$ .

to low entropy states and the first few atomic layers of the surface of such a liquid metal are virtually crystalline. At sufficiently high temperatures, however, this remaining order is destroyed. That is, the surface becomes thermally delocalized and  $\gamma$  reverts to the familiar monotonic decrease with temperature. This phenomenon has also been observed with pure metals, such as Cu, Zn and Co [6].

From Fig. 2 we can see that the  $\text{Au}_{73}\text{Ge}_{27}$  source behaves like most pure metals, displaying a linear decrease of  $V_0$  with  $T$  [3]. It would, therefore, appear that the presence of Si is responsible for the abnormal behaviour of  $\gamma$  with  $T$ , in the case of the  $\text{Au}_{82}\text{Si}_{18}$  and  $\text{Au}_{77}\text{Ge}_{14}\text{Si}_9$  alloys.

We now turn our attention to the mass spectrum of the source (Figs. 3 and 4). It can be seen that the

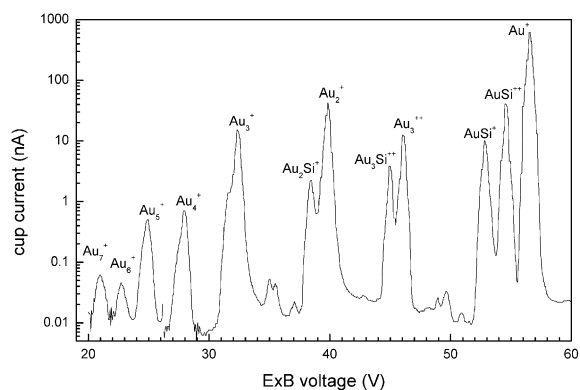


Fig. 4. Portion of  $\text{Au}_{82}\text{Si}_{18}$  mass spectrum rich in ion clusters.

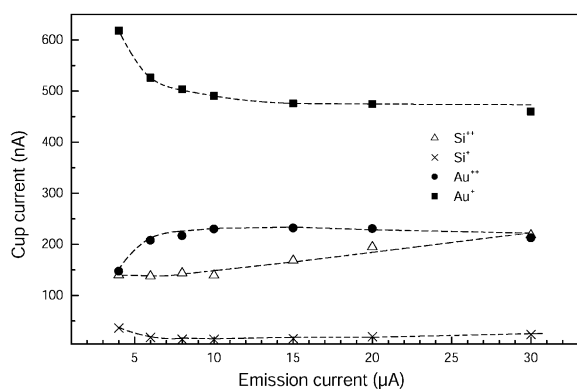


Fig. 5. Intensity of monoatomic ions of  $\text{Au}_{82}\text{Si}_{18}$  source versus emission current,  $i$ .  $T=850^\circ\text{C}$ .

dominant species are  $\text{Au}^+$ ,  $\text{Si}^{2+}$ ,  $\text{Au}^{2+}$  and  $\text{Si}^+$ , in that order; we exclude  $\text{AuSi}^+$ , for the moment, from our discussion. The main  $\text{Si}^{2+}$  peak is due to the  $^{28}\text{Si}$  isotope and the smaller peaks adjacent to it are due to  $^{29}\text{Si}$  and  $^{30}\text{Si}$ . Fig. 5 shows the intensity of the main species emitted versus emission current, whereas in Fig. 6 the ratio of the abundance in the beam of the doubly to singly charged monoatomic ions is shown, as a function of emission current. It is clear that due to space-charge stabilization of the apex field [7,8] above  $10\mu\text{A}$ ,  $I_{2+}/I_+$  remains essentially constant. We now turn to Table 1, where the evaporation fields  $E$  [9], as well as the fields for post ionization  $E_{\text{pi}}$  are shown for both Au and Si [10]. It is seen that  $E_{\text{Si}^{2+}} < E_{\text{Si}^+}$  indicating, according to Brandon's criterion [9], that  $\text{Si}^{2+}$  will dominate in the beam,

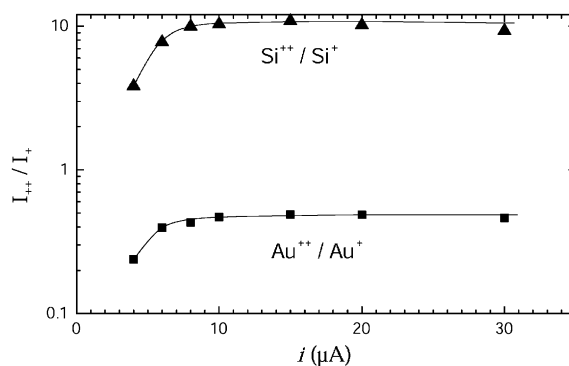


Fig. 6. Ratio ( $I_{2+}/I_+$ ) of the abundance of doubly to singly charged monoatomic ions for  $\text{Au}_{82}\text{Si}_{18}$  source as a function of emission current,  $i$ .  $T=850^\circ\text{C}$ .

Table 1

Values of the evaporation fields calculated for singly ( $E^+$ ) and doubly charged ( $E^{2+}$ ) ions for Au and Si; see Ref.[11] for details. Also shown are values for the post-ionization from the singly to the doubly charged state ( $E_{\text{pi}}$ ) [10]

	$E^+$ ( $\text{V}/\text{\AA}$ )	$E^{2+}$ ( $\text{V}/\text{\AA}$ )	$E_{\text{pi}}(I > 10 \text{ A})$ ( $\text{V}/\text{\AA}$ )
Au	4.8	5.0	3.5 [3.3]
Si	4.5 (4.7)	3.3 (3.4)	2.3 [2.1]

Values in parentheses are given both by Brandon [9] and Ishitani et al. [12]. Values for  $E_{\text{pi}}$  in square brackets are from Ref. [22] for Au and Ref. [23] for Si.

and this is in fact the case. Also, the consistency of  $E_{\text{pi}}$  for Au and  $E_{\text{Si}^{2+}}$  we take as evidence that while  $\text{Si}^{2+}$  is directly field evaporated,  $\text{Au}^{2+}$  forms by the post-ionization of  $\text{Au}^+$ . As a matter of fact, the field has only to change by less than 5% in order to achieve the constant value of  $I_{2+}/I_+ \simeq 0.5$  for Au (Fig. 6, Ref. [10]). We recall that the evaporation field is the field value for which the electric field-reduced potential energy barrier seen by an escaping ion is equal to zero.

Returning now to Figs. 5 and 6, the near constancy of  $I_{2+}/I_+$ , above  $10\mu\text{A}$ , for both Au and Si, as already stated, is due to space-charge stabilization of the apex field. From this point onwards increases in *total current* are effected through increases in emission area, i.e. increases in the number of field-evaporation sites [7,8]. The initial rise in  $I_{2+}/I_+$  up to  $\sim 10\mu\text{A}$  (Fig. 6) is a definite indication that the field increases in this

current range. Since the voltage does not change much from its onset value up to  $\sim 10\mu\text{A}$  ( $<1\%$ ; Fig. 1), field increases can conceivably be achieved through decreases in apex area<sup>1</sup>, and this implies decreases in the number of field-evaporation sites. This self-sharpening of the apex of the liquid emitter eventually comes to a halt, whereupon the opposite starts to occur. Now, if the probability for  $\text{Si}^{2+}$  evaporation increases with increasing field—as it must—then the probability for  $\text{Si}^+$  evaporation will decrease, assuming that both  $\text{Si}^+$  and  $\text{Si}^{2+}$  are emitted from the same atomic evaporation sites. This, combined with the reduction in the number of evaporation sites up to  $\sim 10\mu\text{A}$ , explains the drop in  $\text{Si}^+$  intensity in this current range. In the case of  $\text{Si}^{2+}$ , increases in evaporation rate are obviously offset by decreases in the number of evaporation sites and thus the intensity of  $\text{Si}^{2+}$  is initially constant. For  $i > 10\mu\text{A}$ , the intensities of both  $\text{Si}^+$  and  $\text{Si}^{2+}$  go up (Fig. 5), at almost the same rate, because the emission area increases. In this current range  $I_{2+}/I_+$  for Si remains essentially constant, because the respective probabilities of escape for  $\text{Si}^+$  and  $\text{Si}^{2+}$  remain constant due to the field remaining constant (Fig. 6).

The initial drop in the intensity of  $\text{Au}^+$  and the corresponding increase in the intensity of  $\text{Au}^{2+}$  (Fig. 5) is due to the  $\text{Au}^+$  ions lost through post-ionization to form  $\text{Au}^{2+}$ . This would be consistent with the hypothesis of the field increasing up to about  $10\mu\text{A}$ . With regard to the constancy of the intensity of  $\text{Au}^+$ —and by implication of  $\text{Au}^{2+}$ —above  $10\mu\text{A}$ , presumably, increases in emission area do not affect the number of Au sites as much as in the case of Si. Another possibility is that the increasing angle of emission with current offsets increases in emission current, so that, the on-axis intensities of  $\text{Au}^+$  and  $\text{Au}^{2+}$  remain constant.

Fig. 7 shows the intensity of the ion clusters emitted by the source as a function of current. For comparison, the intensities of  $\text{Au}^+$ ,  $\text{Si}^+$ ,  $\text{Si}^{2+}$ —all believed to be the result of field-evaporation—are also shown.

<sup>1</sup>Alternatively, the length of the ion emitting jet might increase, if indeed a jet exists at the end of the cone-shaped liquid anode for  $i < 10\mu\text{A}$ .

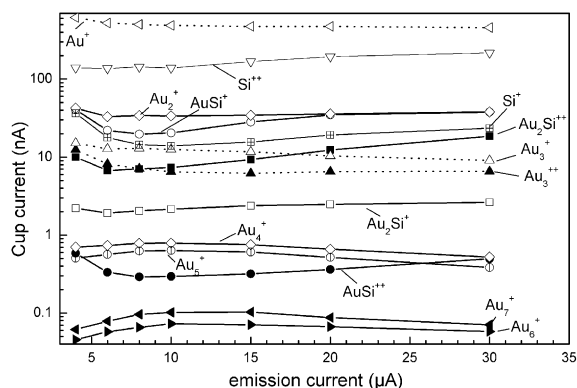


Fig. 7. Intensity of cluster ions of  $\text{Au}_{82}\text{Si}_{18}$  source versus current,  $i$ .  $T=850^\circ\text{C}$ . Also, included for comparison, the intensities of  $\text{Au}^+$ ,  $\text{Si}^+$  and  $\text{Si}^{2+}$ .

It is seen that a clear difference exists in the behaviour of the curves corresponding to clusters made up of a few atoms and those of gold,  $\text{Au}_n$ ,  $n=4-7$ . Can this mean that two different mechanisms are operative in the two cases? The answer is probably yes. The similarity between the curves corresponding to small clusters and those of  $\text{Au}^+$ ,  $\text{Si}^+$  and  $\text{Si}^{2+}$  suggests that they are formed by some kind of surface field-ionization mechanism. Field evaporation is one such mechanism. That this might be so is borne out by the energy distribution measurements of Sudraud et al. [13] and Papadopoulos [14] using pure Au. For  $\text{Au}_2^+$  Papadopoulos finds a primary, sharp peak in the energy distribution, corresponding to ions created at, or near, the surface, with a secondary peak or shoulder appearing at high currents. At  $40\mu\text{A}$  Papadopoulos finds a secondary peak at 20 eV deficit with respect to the primary peak; similarly, the same author finds, with  $\text{Au}_3^{2+}$ , a shoulder appearing at  $\sim 20\mu\text{A}$ , which becomes more profound at  $40\mu\text{A}$ . The shoulder has again an energy deficit  $\sim 70\text{eV}$  with respect to the primary peak. Such large deficits correspond to ions created at some distance from the emitter and are not compatible with a surface field-ionization mechanism. Sudraud et al. operating at high currents, find a similar behaviour for  $\text{Au}_2^+$  and  $\text{Au}_3^+$ . The same authors find deficits of hundreds of electron volts with respect to the  $\text{Au}^+$  peak for  $\text{Au}_4^+$  and  $\text{Au}_5^+$ .

It appears, therefore, that  $\text{Au}_n^+$  clusters,  $n > 7$ , form by a mechanism other than surface field-ionization, away from the emitter. This mechanism is, most probably, one involving the break-up of droplets, possibly by ion capture, as proposed by Hornsey [15]. This may account for the different trend shown by the curves corresponding to heavier Au cluster ions in Fig. 7. In any event, it is highly unlikely that ion clusters containing so many atoms would be field-emitted as a unit. As far as the composite AuSi clusters are concerned, the similarity of the relevant curves (Fig. 7) with those of  $\text{Au}_n^+$ ,  $n = 1-3$ ,  $\text{Si}^+$  and  $\text{Si}^{2+}$  supports a surface field-ionization mechanism for their creation. On the other hand, the curves of Fig. 8 tend to mitigate such a hypothesis. It is impossible for  $I_{2+}/I_+$  to go down with increasing electric field in a field-assisted thermal evaporation process; it can only go up under conditions of constant temperature. This, however, holds true in the case where both the singly and doubly charged ions emerge from the same sites; in the case of cluster ions the notion of an atomic emission site is meaningless. Thus, experimental results remain inconclusive as to the exact mechanism of creation of cluster ions containing a few atoms. This brings us to the work of Joyes and Van der Walle [16]. According to these authors, two types of droplet break-up mechanism co-exist. In the first mechanism,

droplets charged above the Rayleigh limit [17] disintegrate almost immediately after emission, thus giving rise to peak energy deficits corresponding to cluster ion creation at, or near, the surface. This mechanism liberates small clusters and neutral atoms close to the apex of the liquid anode. We recall that Rayleigh's criterion [17] essentially states that a spherical drop will become unstable, without deviating from sphericity, when the outwards electric stress on its surface exceeds the inward stress due to surface tension. In the second mechanism, large metastable droplets, being lightly charged, would have longer lifetimes but would eventually break up at some distance from the emitter, under the influence of their thermal energy. This process would tend to produce larger clusters and energy deficits. These two mechanisms may account for the differences seen in Fig. 7 for clusters with  $n > 7$  and those containing only two to three atoms.

Finally, we present energy distribution measurements for the  $\text{Si}^+$  and  $\text{Si}^{2+}$  ions (Figs. 9, 10). We can see that for  $\text{Si}^+$  the curves are distorted as found by Swanson [18] with a  $\text{Au}_{90}\text{Si}_{10}$  LMAs (m.p.  $657^\circ\text{C}$ ), for currents between 5 and  $-25\mu\text{A}$ . In fact, the curve for  $5\mu\text{A}$  looks very much like Swanson's, although the width of his curve is larger than ours. Also, as with Swanson's results, the shoulder tends to disappear as the current is

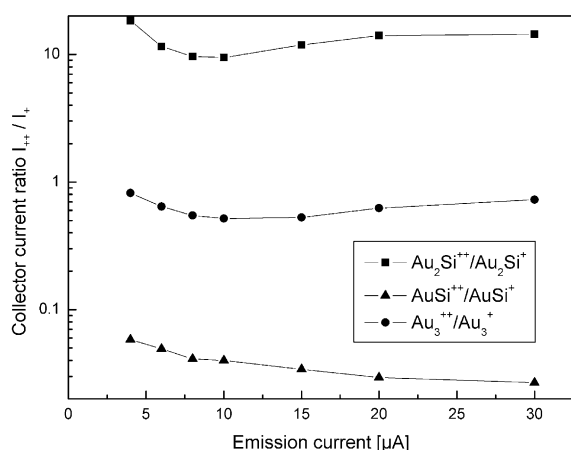


Fig. 8. Ratio ( $I_{2+}/I_+$ ) of the abundance of doubly to singly charged cluster ions for  $\text{Au}_{82}\text{Si}_{18}$  source versus emission current,  $i$ .  $T = 850^\circ\text{C}$ .

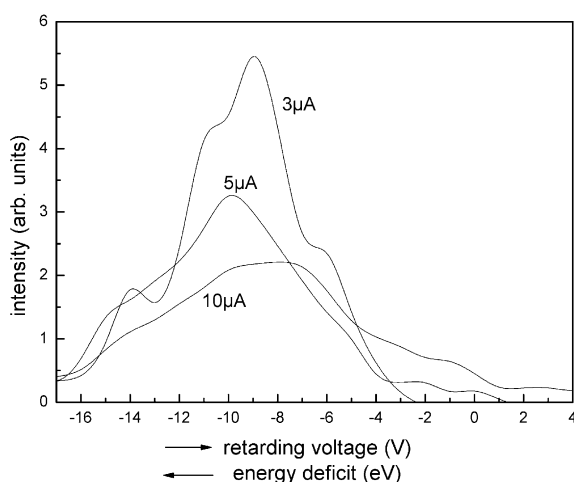


Fig. 9. Energy distribution of  $\text{Si}^+$  ions versus emission current.  $T = 734^\circ\text{C}$ .

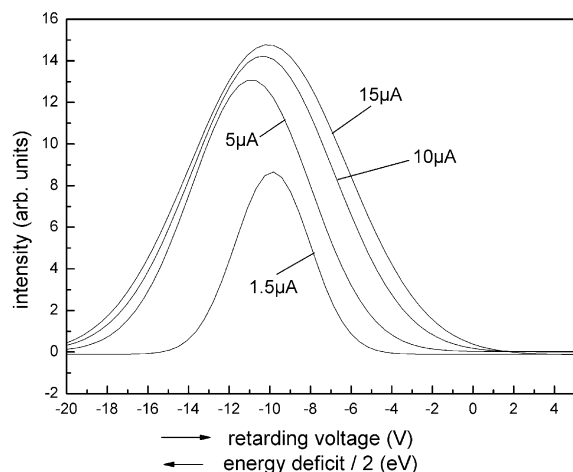


Fig. 10. Energy distribution of  $\text{Si}^{2+}$  ions versus emission current.  $T = 734^\circ\text{C}$ .

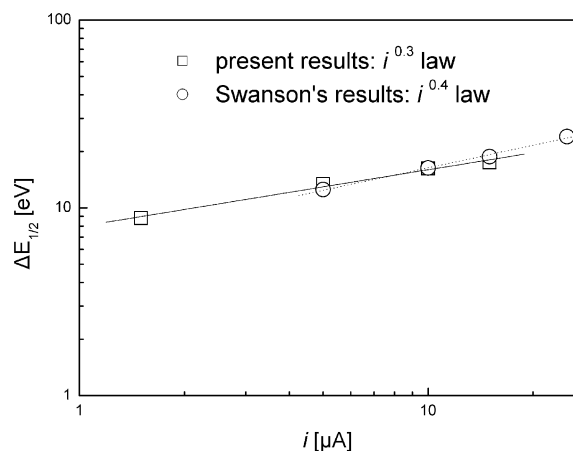


Fig. 11. Energy spread  $\Delta E_{1/2}$  (FWHM) of  $\text{Si}^{2+}$  ions versus  $i$ ;  $T = 734^\circ\text{C}$  ( $\square$ ). Also shown results of Swanson's [18]  $\text{Au}_{90}\text{Si}_{10}$  source ( $\circ$ );  $T = 660^\circ\text{C}$ . Note that Swanson's results refer to voltage rather than energy spread measurements, so that for doubly charged ions like  $\text{Si}^{2+}$  they were multiplied by a factor of 2.

raised. However, our values for the energy spread ( $\Delta E_{1/2}$ ) of  $\text{Si}^{2+}$  are very close to those of Swanson (Fig. 11). Our results display a  $\Delta E \propto i^{1/3}$  relationship, in exact agreement with the  $\text{Si}^{2+}$  results of our  $\text{Au}_{77}\text{Ge}_{14}\text{Si}_9$  source [19].

The first thing that comes to mind about the nature of the secondary peaks, or shoulders in the energy distribution of  $\text{Si}^{2+}$  is a mechanism of field

Table 2

Comparison of experimentally and theoretically obtained values of the peak energy deficit  $\Delta E$  (eV) for  $\text{Si}^+$  and  $\text{Si}^{2+}$ .

	Exp. $\Delta E(n)$ (eV)	Theor. $\Delta E(n)$ (eV)
$\text{Si}^+$	8.9	7.9 (8.1)
$\text{Si}^{2+}$	19.6	19.4 (19.4)

Values in parentheses are for values of  $\Lambda$  and  $\phi_C$  from Refs. [9,12].

ionization at some distance from the emitter. However, there are serious difficulties with this explanation, due to insufficient heat input to the emitter to account for the necessary atom flux to be field-ionized [20]—unless, as in the case of some cluster ions, the atoms are released from the break-up of larger ionic complexes or droplets, possibly by ion impact.

Table 2 shows the calculated peak energy deficits ( $\Delta E(n)$ ), according to [21]

$$\Delta E(n) = \Lambda + \sum_n I_n - n\phi_C \quad (2)$$

and compares them to those found experimentally for low currents. In Eq. (2)  $\Lambda$  is the binding energy (heat of evaporation) of the bound atom (subsequently ion);  $\sum_n I_n$  is the sum of the ionization potentials, if the atom is  $n$ -fold ionized;  $\phi_C$  is the work function of the retarding electrode (4.9 eV for Ni) [24]. It is seen (Table 2) that the agreement between theory and experiment is quite satisfactory, adding support to our notion that a field evaporation mechanism is responsible for the creation of  $\text{Si}^{2+}$  ions, as well as being the primary emission mechanism in the case of  $\text{Si}^+$ .

## Acknowledgements

C.J. Aidinis, G.L.R. Mair, C.A. Londos and Th. Ganetsos thank the Rossendorf Research Centre, for extended visits. Thanks are also due to Prof. W. Möller for his interest and support. We thank Dr. D.R. Kingham for communicating to us his post-ionization calculations. C.J. Aidinis acknowledges financial support from the University of Athens Special Account for Research Grants.

**References**

- [1] F. Machelet, R. Mühle, I. Stiebritz, *J. Phys. D: Appl. Phys.* 20 (1987) 1417.
- [2] G.L.R. Mair, *Vacuum* 36 (1986) 365.
- [3] G.L.R. Mair, *Nucl. Instrum. Methods* 172 (1980) 567.
- [4] L. Bischoff, J. Teichert, Th. Ganetsos, G.L.R. Mair, *J. Phys. D* 33 (2000) 692.
- [5] C.J. Smithells, *Metal Reference Book*, 5th Edition, Butterworth, London, 1976.
- [6] C.A. Croxton, *Statistical Mechanics of the Liquid Surface*, Wiley, Chichester, 1980 p. 161.
- [7] D.R. Kingham, L.W. Swanson, *Appl. Phys. A* 34 (1984) 123.
- [8] G.L.R. Mair, R.G. Forbes, *J. Phys. D* 24 (1991) 22.
- [9] D.G. Brandon, *Surf. Sci.* 3 (1964) 1.
- [10] D.R. Kingham, private communication to G.L.R. Mair; D.R. Kingham, *Surf. Sci.* 116 (1982) 273.
- [11] G.L.R. Mair, Th. Ganetsos, L. Bischoff, J. Teichert, *J. Phys. D* 33 (2000) L86.
- [12] T. Ishitani, K. Umemura, Y. Kawayami, *J. Vac. Sci. Technol. B* 6 (1988) 931.
- [13] P. Sudraud, C. Collier, J. Van der Walle, *J. Phys.* 40 (1979) L207.
- [14] S. Papadopoulos, D. Phil. Thesis, Oxford University, 1986; S. Papadopoulos, D.L. Barr, W. Brown, *J. Phys.* 47 (1986) C2-101.
- [15] R. Hornsey, T. Ishitani, *Jpn. J. Appl. Phys.* 29 (1990) 2116.
- [16] P. Joyes, J. Van de Walle, *J. Phys.* 47 (1986) 21.
- [17] Lord Rayleigh, *Philos. Mag.* 14 (1882) 184.
- [18] L.W. Swanson, *Nucl. Instrum. Methods.* 218 (1983) 341.
- [19] G.L.R. Mair, L. Bischoff, A.W.R. Mair, C.J. Aidinis, Th. Ganetsos, C.A. Aleiev, *J. Phys. D* 35 (2002) L33.
- [20] P.D. Prewett, G.L.R. Mair, *Focused Ion Beams from Liquid Metal Ion Sources*, Research Studies Press, Taunton, UK, 1991.
- [21] R.G. Forbes, *Surf. Sci.* 61 (1976) 221.
- [22] D.R. Kingham, *Appl. Phys. A* 31 (1983) 161.
- [23] L.W. Swanson, D.R. Kingham, *Appl. Phys. A* 41 (1986) 223.
- [24] M. Von Ardenne, *Tabellen zur angewandten Physik* 1Bd, Berlin, 1979, p. 75.